

SPACE-TIME DISCONTINUOUS GALERKIN METHOD FOR THE COMPRESSIBLE NAVIER-STOKES EQUATIONS ON DEFORMING MESHES

J.J.W. van der Vegt*, C.M. Klaij*, F. van der Bos*, and H. van der Ven†

*University of Twente, Department of Applied Mathematics
P.O. Box 217, 7500 AE Enschede, The Netherlands
e-mails: [j.j.w.vandervegt, c.m.klaij, f.vanderbos}@math.utwente.nl](mailto:{j.j.w.vandervegt, c.m.klaij, f.vanderbos}@math.utwente.nl)

†National Aerospace Laboratory NLR,
P.O. Box 90502, 1006 BM Amsterdam, The Netherlands
e-mail: venvd@nlr.nl

Key words: Space-time discontinuous Galerkin methods, finite element methods, deforming meshes, pseudo-time integration, compressible Navier-Stokes equations

Abstract. *An overview is given of a space-time discontinuous Galerkin finite element method for the compressible Navier-Stokes equations. This method is well suited for problems with moving (free) boundaries which require the use of deforming elements. In addition, due to the local discretization, the space-time discontinuous Galerkin method is well suited for mesh adaptation and parallel computing. The algorithm is demonstrated with computations of the unsteady flow field about a delta wing and a NACA0012 airfoil in rapid pitch up motion.*

1 INTRODUCTION

The accurate numerical simulation of fluid-structure interaction is important in aerodynamics. Examples are wing flutter, control devices and the flow about helicopter rotors. In all of these cases one encounters unsteady flows with complicated flow structures, such as vortices which interact with each other and need to be captured over long distances, flow separation and shocks, but one also has to deal with moving and deforming meshes to accommodate for the boundary motion. The use of dynamic meshes, however, significantly complicates the numerical discretization since special care has to be given to ensure a conservative and accurate numerical discretization. A detailed discussion of the complications of using time dependent meshes for finite volume and finite element methods can be found in e.g. [7, 12].

An excellent frame work to solve flow problems on time dependent domains is to consider them in space-time. The problem is then discretized directly in four dimensional space using for instance a Galerkin least squares or a discontinuous Galerkin (DG) finite

element method. In particular, discontinuous Galerkin methods are very attractive because they use a very compact discretization which is conservative and well suited for local mesh refinement and/or the adjustment of the polynomial order in each element (*hp*-adaptation). In addition, the method is very efficient on parallel computers. Detailed surveys of DG methods applied to hyperbolic, (incompletely) parabolic and elliptic problems can be found in [1, 3, 4, 5, 6].

In this paper an overview is given of the space-time DG method for the compressible Navier-Stokes equations and the algorithm is demonstrated with several aerodynamical applications. The space-time DG technique discussed in this paper was originally developed for the Euler equations of gas dynamics in [15, 16] and applied to a variety of aerodynamical applications, such as rotorcraft [2] and deforming wings [17]. Recently, the space-time DG method has been extended to the compressible Navier-Stokes equations and applied to vortex dominated flows, including dynamic stall problems, which require the use of locally refined and deforming meshes [8]. A complete *hp*-error and stability analysis of the space-time DG discretization for the advection-diffusion equation is given in [14].

The space-time discretization results in an implicit time discretization which requires the solution of a large system of nonlinear equations. This can be done either with a Newton type method or using a pseudo-time stepping technique. In the pseudo-time stepping method the nonlinear algebraic equations are solved by adding a pseudo-time derivative of the unknown expansion coefficients in the DG discretization and marching the equations to steady state in pseudo-time using a Runge-Kutta time integration scheme. This technique has as main benefit that it preserves the locality of the discontinuous Galerkin method and was initially applied to the space-time DG discretization of the Euler equations of gas dynamics in combination with a multigrid method in [15]. Recently, the pseudo-time integration method has been extended to space-time discretizations of the compressible Navier-Stokes equations in [9] by reducing the serious time step limitation due to the viscous contribution.

The outline of this paper is as follows. In Section 2 we summarize the Navier-Stokes equations describing compressible viscous flows. The space-time DG discretization is discussed in Section 3 and the pseudo-time integration technique to solve the resulting algebraic equations in Section 4. Several applications are discussed in Section 5 and concluding remarks are drawn in Section 6. For complete details of the algorithms discussed in this paper we refer to [8, 9, 10, 15, 16].

2 COMPRESSIBLE NAVIER-STOKES EQUATIONS

We consider the compressible Navier-Stokes equations in an open domain $\mathcal{E} \subset \mathbb{R}^4$. The flow domain $\Omega(t)$ at time t is defined as $\Omega(t) := \{\bar{x} \in \mathbb{R}^3 : (t, \bar{x}) \in \mathcal{E}\}$, where the point with position $\bar{x} = (x_1, x_2, x_3)$ at time $t = x_0$ has Cartesian coordinates $x = (x_0, x_1, x_2, x_3)$. The space-time domain boundary consists of $\mathcal{Q} := \{x \in \partial\mathcal{E} : t_0 < x_0 < T\}$ and the spatial domains at the initial and final time t_0 and T , viz. $\Omega(t_0) := \{x \in \partial\mathcal{E} : x_0 = t_0\}$

and $\Omega(T) := \{x \in \partial\mathcal{E} : x_0 = T\}$. Using this notation, the compressible Navier-Stokes equations can be written in conservation form as:

$$\begin{cases} U_{i,0} + F_{ik}^e(U)_{,k} - F_{ik}^v(U, \nabla U)_{,k} = 0 & \text{on } \mathcal{E}, \\ U = U_0 & \text{at } \Omega(t_0), \\ U = \mathcal{B}(U, U^b) & \text{at } \mathcal{Q}, \end{cases}$$

with $U \in \mathbb{R}^5$ the vector of conservative variables, $F^e \in \mathbb{R}^{5 \times 3}$ the inviscid flux, $F^v \in \mathbb{R}^{5 \times 3}$ the viscous flux, $U_0 \in \mathbb{R}^5$ the initial flow field and $\mathcal{B} \in \mathbb{R}^5$ the boundary operator with U^b the prescribed boundary data. The summation convention on repeated indices is used with $i = 1, \dots, 5$ and $k = 1, 2, 3$ and a comma denotes differentiation with respect to the indicated Cartesian coordinate direction.

The conservative variables and the inviscid and viscous fluxes are defined as:

$$U = \begin{bmatrix} \rho \\ \rho u_j \\ \rho E \end{bmatrix}, \quad F_k^e = \begin{bmatrix} \rho u_k \\ \rho u_j u_k + p \delta_{jk} \\ u_k(\rho E + p) \end{bmatrix}, \quad F_k^v = \begin{bmatrix} 0 \\ \tau_{jk} \\ \tau_{kj} u_j - q_k \end{bmatrix},$$

with ρ the density, ρu the momentum density vector, ρE the total energy density, p the pressure, δ the Kronecker delta function. The shear stress tensor τ is defined as:

$$\tau_{jk} = -\frac{2}{3}\mu u_{i,i} \delta_{jk} + \mu(u_{j,k} + u_{k,j}),$$

with $i = 1, 2, 3$ and the dynamic viscosity coefficient μ given by Sutherland's law:

$$\frac{\mu}{\mu_\infty} = \frac{T_\infty + T_S}{T + T_S} \left(\frac{T}{T_\infty} \right)^{3/2},$$

where T is the temperature, T_S a constant and $(\cdot)_\infty$ denotes free-stream values. The heat flux vector q is defined as:

$$q_k = -\kappa T_{,k},$$

with κ the thermal conductivity coefficient. For a calorically perfect gas, the pressure p , internal energy e and temperature T are given by the following equations of state:

$$p = \rho R T, \quad e = c_v T, \quad T = \frac{1}{c_v} \left(E - \frac{1}{2} u_i u_i \right)$$

where $R = c_p - c_v$ is the specific gas constant and c_p and c_v the specific heats at constant pressure and constant volume, respectively.

The viscous flux F^v is homogeneous with respect to the gradient of the conservative variables ∇U . This defines the homogeneity tensor $A \in \mathbb{R}^{5 \times 3 \times 5 \times 3}$ as:

$$A_{ikrs}(U) = \frac{\partial F_{ik}^v(U, \nabla U)}{\partial (U_{r,s})}.$$

This property is essential for the treatment of the viscous terms in the space-time formulation of the compressible Navier-Stokes equations [8].

3 SPACE-TIME DISCRETIZATION

The space-time discretization starts with the tessellation $\mathcal{T}_h^n = \{\mathcal{K}\}$ in a space-time slab, which is the flow domain \mathcal{E} in the time interval (t_n, t_{n+1}) . The associated function spaces are defined as:

$$\begin{aligned} W_h &:= \{W \in (L^2(\mathcal{E}_h))^5 : W|_{\mathcal{K}} \circ G_{\mathcal{K}} \in (P^m(\hat{\mathcal{K}}))^5, \quad \forall \mathcal{K} \in \mathcal{T}_h\}, \\ V_h &:= \{V \in (L^2(\mathcal{E}_h))^{\mathbb{5} \times \mathbb{3}} : V|_{\mathcal{K}} \circ G_{\mathcal{K}} \in (P^m(\hat{\mathcal{K}}))^{\mathbb{5} \times \mathbb{3}}, \quad \forall \mathcal{K} \in \mathcal{T}_h\}, \end{aligned}$$

where $G_{\mathcal{K}}$ denotes the mapping of the master element $\hat{\mathcal{K}} = (-1, 1)^4$ to element \mathcal{K} and $P^m(\hat{\mathcal{K}})$ denotes the space of polynomials of degree at most m . The set of internal faces in a space-time slab is denoted by \mathcal{S}_I^n and the set of boundary faces by \mathcal{S}_B^n . The traces from the left and right are denoted by $(\cdot)^L$ and $(\cdot)^R$, respectively. The average operator is defined as $\{\!\!\{ \cdot \}\!\!\} = 1/2((\cdot)^L + (\cdot)^R)$ and the jump operator as $[\![\cdot]\!]_k = (\cdot)^L n_k^L + (\cdot)^R n_k^R$, with n the outward normal vector of the element under consideration. Using this notation, the weak formulation of the compressible Navier-Stokes equations can be written as follows.

Find a $U \in W_h$, such that for all $W \in W_h$:

$$\begin{aligned} & - \sum_{\mathcal{K} \in \mathcal{T}_h^n} \int_{\mathcal{K}} (W_{i,0} U_i + W_{i,k} (F_{ik}^e - A_{ikrs} U_{r,s} + \mathcal{R}_{ik})) d\mathcal{K} \\ & + \sum_{K \in \mathcal{T}_h^n} \left(\int_{K(t_{n+1}^-)} W_i^L U_i^L dK - \int_{K(t_n^+)} W_i^L U_i^R dK \right) \\ & + \sum_{\mathcal{S} \in \mathcal{S}_I^n} \int_{\mathcal{S}} (W_i^L - W_i^R) H_i d\mathcal{S} + \sum_{\mathcal{S} \in \mathcal{S}_B^n} \int_{\mathcal{S}} W_i^L H_i^b d\mathcal{S} \\ & - \sum_{\mathcal{S} \in \mathcal{S}_I^n} \int_{\mathcal{S}} [\![W_i]\!]_k \{\!\!\{ A_{ikrs} U_{r,s} - \eta \mathcal{R}_{ik}^S \}\!\!\} d\mathcal{S} \\ & - \sum_{\mathcal{S} \in \mathcal{S}_B^n} \int_{\mathcal{S}} W_i^L (A_{ikrs}^b U_{r,s}^b - \eta \mathcal{R}_{ik}^S) \bar{n}_k^L d\mathcal{S} = 0. \end{aligned}$$

Here, $H(U^L, U^R) \in \mathbb{R}^5$ is the inviscid numerical flux from the HLLC approximate Riemann solver with the extension needed for moving meshes (cf. [15]) and $(\cdot)^b$ indicates dependence on the prescribed boundary data. The stability constant η must satisfy the condition $\eta > N_f$, with N_f the number of faces per element. The local lifting operator is denoted by $\mathcal{R}^S \in \mathbb{R}^{\mathbb{5} \times \mathbb{3}}$ and defined [8] as:

Find an $\mathcal{R}^S \in V_h$, such that for all $V \in V_h$:

$$\sum_{\mathcal{K} \in \mathcal{T}_h^n} \int_{\mathcal{K}} V_{ik} \mathcal{R}_{ik}^S d\mathcal{K} = \begin{cases} \int_{\mathcal{S}} \{\!\!\{ V_{ik} A_{ikrs} \}\!\!\} [\![U_r]\!]_s d\mathcal{S} & \text{for } \mathcal{S} \in \mathcal{S}_I^n, \\ \int_{\mathcal{S}} V_{ik}^L A_{ikrs}^L (U_r^L - U_r^b) \bar{n}_s d\mathcal{S} & \text{for } \mathcal{S} \in \mathcal{S}_B^n, \end{cases}$$

The global lifting operator $\mathcal{R} \in \mathbb{R}^{5 \times 3}$ is obtained from the local lifting operator \mathcal{R}^S using the relation:

$$\mathcal{R} = \sum_{S \in \mathcal{S}_I^n \cup \mathcal{S}_B^n} \mathcal{R}^S.$$

The upwind character of the numerical time-flux in the integrals over the time faces $K(t_n^+)$ and $K(t_{n+1}^-)$ ensures causality in time. The trial function U and the test function W in each element $\mathcal{K} \in \mathcal{T}_h^n$ are represented as polynomials:

$$U(t, \bar{x})|_{\mathcal{K}} = \hat{U}_j \psi_j(t, \bar{x}), \quad \text{and} \quad W(t, \bar{x})|_{\mathcal{K}} = \hat{W}_l \psi_l(t, \bar{x}),$$

with $(\hat{\cdot})$ the expansion coefficients and ψ the basis functions described in [8]. The system of algebraic equations for the expansion coefficients of U is obtained by replacing U and W in the weak formulation with their polynomial expansions and using the fact that the test functions W are arbitrary. For each physical time step the system can be written as:

$$\mathcal{L}(\hat{U}^n; \hat{U}^{n-1}) = 0, \tag{1}$$

and the algorithm is unconditionally stable with respect to the physical time step $\Delta t = t_{n+1} - t_n$.

4 PSEUDO-TIME STEPPING METHODS

The solution of the system of non-linear algebraic equations (1) is a non-trivial task. It consists of $5N_e N_p$ equations, with N_e the number of elements and N_p the number of degrees of freedom per element. Essentially, two main techniques are available for the solution of this nonlinear system, a Newton method, which (approximately) linearizes the equations and solves the nonlinear equations iteratively, or a pseudo-time integration method. In the pseudo-time integration method we add a pseudo-time derivative to (1):

$$\frac{\partial \hat{U}}{\partial \tau} = -\frac{1}{\Delta t} \mathcal{L}(\hat{U}; \hat{U}^{n-1}),$$

and iterate in pseudo-time τ to a steady-state using Runge-Kutta methods. At steady-state we have $\hat{U}^n = \hat{U}$.

The key benefit of this approach is that the discretization maintains the same local structure as the original space-time DG method, which is beneficial for parallel computing, and no large global linear system needs to be solved. In particular, when combined with an efficient multigrid technique and using optimized coefficients in the Runge-Kutta method, this results in an efficient algorithm to solve the algebraic equations in space-time DG discretizations, as outlined in [15] for the Euler equations. For the compressible Navier-Stokes equations one encounters, however, locally in viscous dominated regions a serious pseudo-time step restriction. This would significantly reduce the efficiency of the

numerical algorithm, but in [9] it is demonstrated that by using the family of Runge-Kutta methods proposed by Kleb e.a. [11] it is possible to significantly alleviate this pseudo-time step restriction. Combining the Runge-Kutta schemes for the inviscid and viscous flow regimes then results in an efficient pseudo-time integration method for viscous compressible flows, which can be further improved using a multigrid convergence acceleration technique [10].

The pseudo-time algorithm is an explicit five stage Runge-Kutta method in inviscid flow regions, which has optimized coefficients to ensure maximal damping of the transients and a large stability domain, see [15]. This algorithm is combined with the Melson correction [13] to enhance the stability of the pseudo-time integration when the pseudo-time step is close to the physical time step.

This scheme is labelled as the EXI scheme and can be summarized as:

1. Initialize $\hat{V}^0 = \hat{U}$.
2. For all stages $s = 1$ to 5 compute \hat{V}^s as:

$$(I + \alpha_s \lambda I) \hat{V}^s = \hat{V}^0 + \alpha_s \lambda (\hat{V}^{s-1} - \mathcal{L}(\hat{V}^{s-1}; \hat{U}^{n-1})).$$

3. Return $\hat{U} = \hat{V}^5$.

The Runge-Kutta coefficients at stage s are denoted by α_s and defined as: $\alpha_1 = 0.0791451$, $\alpha_2 = 0.163551$, $\alpha_3 = 0.283663$, $\alpha_4 = 0.5$ and $\alpha_5 = 1.0$. The matrix I represents the identity matrix. The factor λ is the ratio between the pseudo-time step $\Delta\tau$ and the physical time step: $\lambda = \Delta\tau/\Delta t$. The Melson correction consists in treating \hat{V} semi-implicitly, without this the scheme would become unstable for values of λ around one.

In the viscous dominated part of the flow domain we use the explicit four stage Runge-Kutta method proposed by Kleb e.a. [11]. This algorithm has a very large stability domain along the negative real axis which significantly enhances the stability in flow regions where viscosity is dominant.

The method is labeled as the EXV scheme and can be summarized as:

1. Initialize $\hat{V}^0 = \hat{U}$.
2. For all stages $s = 1$ to 4 compute \hat{V}^s as:

$$\hat{V}^s = \hat{V}^0 - \alpha_s \lambda \mathcal{L}(\hat{V}^{s-1}; \hat{U}^{n-1}).$$

3. Return $\hat{U} = \hat{V}^4$.

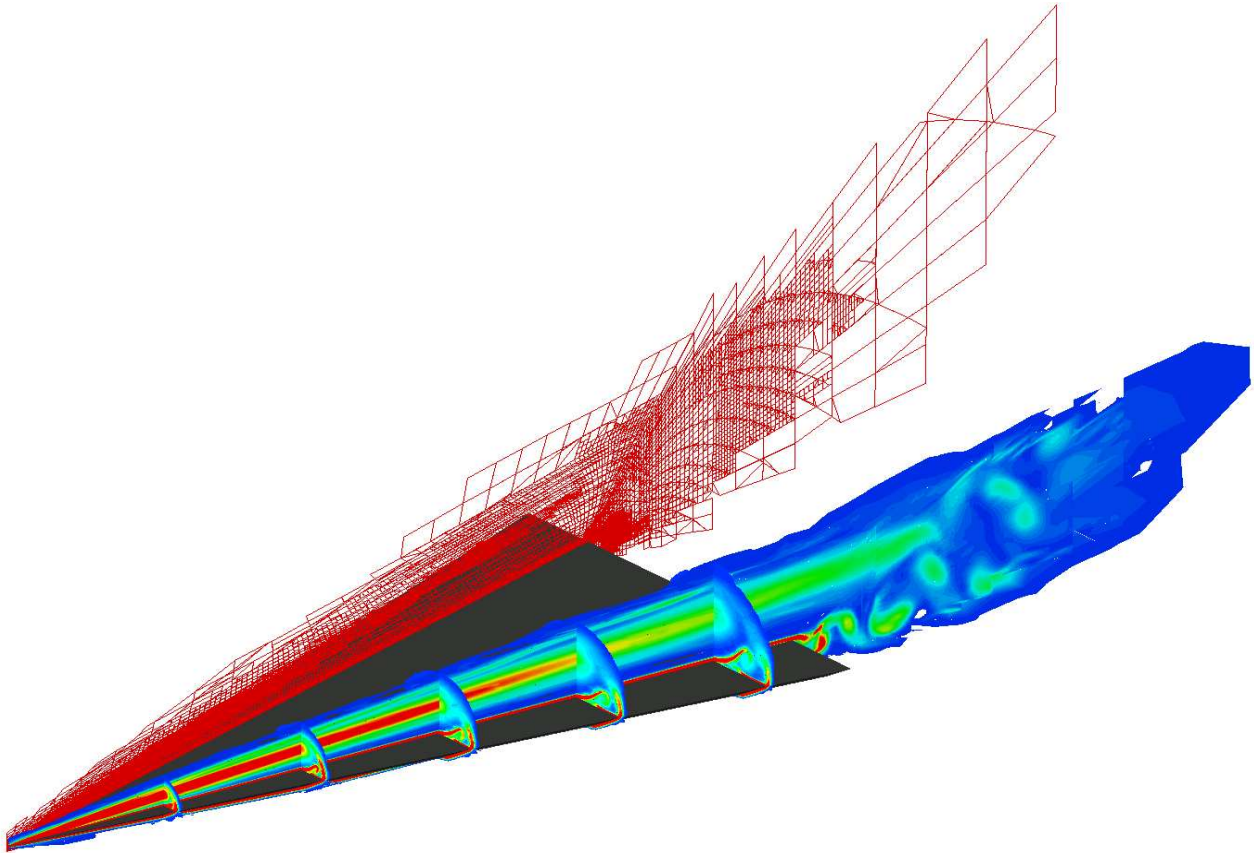


Figure 1: Adapted mesh and vorticity field in primary vortex and cross-sections of a delta wing at $Re_c = 100.000$, $Ma = 0.3$ and $\alpha = 12.5$ degrees.

The Runge-Kutta coefficients at stage s are defined as: $\alpha_1 = 0.0178571$, $\alpha_2 = 0.0568106$, $\alpha_3 = 0.174513$ and $\alpha_4 = 1$. The EXV Runge-Kutta scheme does not require the use of the Melson correction to ensure stability for small values of λ .

The performance of the pseudo-time integration method is enhanced by using the maximum possible pseudo-time step in each element. This time step depends on both the CFL and diffusion number and is estimated using Fourier analysis for the advection-diffusion equation. This also determines which of the schemes, either EXI or EXV, is locally applied. For details on this switching algorithm we refer to [9].

5 RESULTS

As a first application we consider the unsteady flow about a delta wing with sharp leading edges. At the rear the delta wing is closed with a blunt trailing edge. The flow

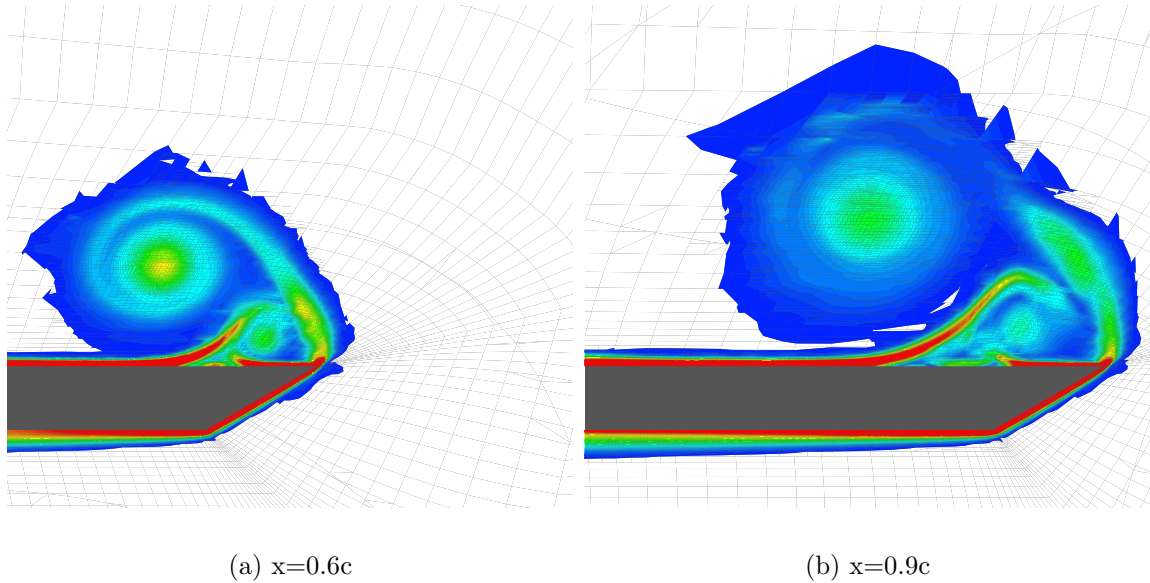


Figure 2: Vorticity field near leading edge of delta wing ($Re_c = 100.000$, $Ma = 0.3$ and $\alpha = 12.5$ degrees).

conditions are a Reynolds number based on the chord length $Re_c = 100.000$, a Prandtl number of $Pr = 0.72$ and a Mach number $Ma = 0.3$. The angle of attack is 12.5 degrees. Under these conditions the flow is turbulent. A Smagorinsky eddy viscosity model has been used to simulate unresolved turbulent flow structures. For this an eddy-viscosity term $\mu_e = \rho(c_s\Delta)|S|$, with $|S| = \sqrt{S_{ij}S_{ij}/2}$ the rate-of-strain magnitude, is added to the dynamic viscosity coefficient in the momentum equation. This term is then treated as a constant in each element in order to maintain the locality of the method. The Smagorinsky constant c_s is set to 0.075, while for the filter-width Δ the typical length of an element is used.

The computations are performed on a locally refined mesh with 1.919.489 active cells, where the adaptation is controlled based on the vorticity in the flow field. A cross-section of the mesh along the primary vortex above the delta wing is shown in Figure 1. Also shown is the vorticity field in several cross-sections. Initially, the flow field is conical, but further downstream secondary and tertiary vortices appear due to flow separation in the boundary layer below the primary and secondary vortices. These features are well captured by the locally refined mesh, see Figure 2. Due to the blunt trailing also an unsteady periodic vortex street is generated in the wake, which is visible in Figure 1.

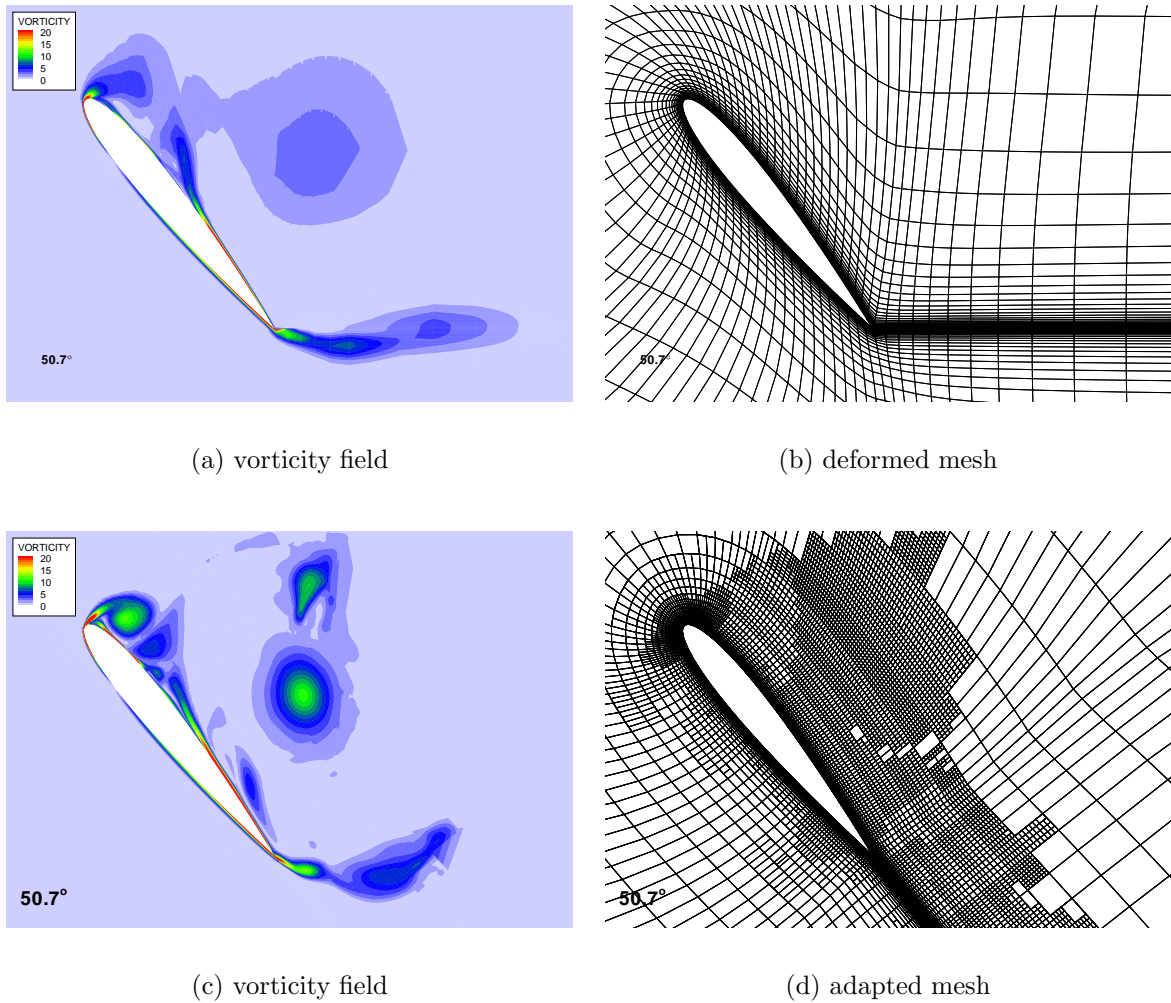


Figure 3: Vorticity field and deformed and adapted meshes around a NACA0012 airfoil at an angle of attack of 50.7 degrees in a laminar dynamic stall simulation ($Re_c = 10000$, $Ma = 0.2$, $Pr = 0.72$).

The second example is the laminar flow about a NACA0012 airfoil in rapid pitch up motion. The flow field is initially attached, but with increasing angle of attack flow separation near the leading edge occurs and finally a large unsteady separation area develops at the lee side of the airfoil, together with vortex shedding from the trailing edge. The computations are done using a deforming and also a locally refined mesh. Both the vorticity field and the meshes are shown in Figure 3. It is apparent that the local mesh refinement significantly improves the capturing of the unsteady vortices, which is not possible on the unadapted mesh since this only has sufficient mesh resolution near the airfoil surface.

6 CONCLUSIONS

A survey of a space-time discontinuous Galerkin finite element method for the compressible Navier-Stokes equations has been given. The algorithm is capable of dealing with deformed and locally refined meshes, which makes it suitable for fluid structure interaction problems and significantly increases the accuracy in capturing important flow structures. High Reynolds number turbulent flows are simulated using large eddy simulation with a Smagorinsky subgrid model. Future work will concentrate on further improving the computational efficiency of the algorithm using the newly developed multigrid method and applying the algorithm to unsteady flow simulations, in particular helicopter rotors in forward flight.

ACKNOWLEDGEMENT

This research has been conducted in the STW project TWI.5541, entitled *Advanced simulation techniques for vortex dominated flows in aerodynamics*. The financial support from STW and the National Aerospace Laboratory NLR is gratefully acknowledged.

REFERENCES

- [1] D. Arnold, F. Brezzi, B. Cockburn, and D. Marini. Unified analysis of discontinuous Galerkin methods for elliptic problems. *SIAM J. Numer. Anal.*, 39:1749–1779, 2002.
- [2] O.J. Boelens, H. van der Ven, B. Oskam, and A.A. Hassan. The boundary conforming discontinuous Galerkin finite element approach for rotorcraft simulations. *J. of Aircraft*, 39(5):776–785, 2002.
- [3] B. Cockburn. Discontinuous Galerkin methods for convection-dominated problems. In T.J. Barth and H. Deconinck, editors, *Lect. Notes in Comp. Sci. and Eng.*, volume 9. Springer Verlag, 1999.
- [4] B. Cockburn. Discontinuous Galerkin methods. *ZAMM Z. Angew. Math. Mech.*, 11:731–754. 65–02, 2003.
- [5] B. Cockburn, G.E. Karniadakis, and C.-W. Shu (Eds.). Discontinuous Galerkin methods. Theory, computation and applications. *Lect. Notes in Comp. Sci. and Eng. (Springer Verlag, 2000)*, 11, 2000.
- [6] B. Cockburn and C.-W. Shu. Runge-Kutta discontinuous Galerkin methods for convection-dominated problems. *J. Sci. Comput.*, 16(3):173–261, 2001.
- [7] C. Farhat, P. Geuzaine, and C. Grandmont. The discrete geometric conservation law and the nonlinear stability of ALE schemes for the solution of flow problems on moving grids. *J. Comput. Phys.*, 174(2):669–694, 2001.

- [8] C.M. Klaij, J.J.W. van der Vegt, and H. van der Ven. A space-time discontinuous Galerkin discretization for the compressible Navier-Stokes equations. *J. Comput. Phys. (in press)*, 2006.
- [9] C.M. Klaij, J.J.W. van der Vegt, and H. van der Ven. Pseudo-time stepping methods for space-time discontinuous Galerkin discretizations of the compressible Navier-Stokes equations. *J. Comput. Phys. (in press)*, 2006.
- [10] C.M. Klaij, M.H. van Raalte, J.J.W. van der Vegt, and H. van der Ven. *hp*-multigrid for space-time discontinuous Galerkin discretizations of the compressible Navier-Stokes equations. *in preparation for J. Comput. Phys.*
- [11] W.L. Kleb, W.A. Wood, and B. van Leer. Efficient Multi-Stage Time Marching for Viscous Flows via Local Preconditioning. *AIAA J.*, 99-3267:181–194, 1999.
- [12] M. Lesoinne and C. Farhat. Geometric conservation laws for flow problems with moving boundaries and deformable meshes, and their impact on aeroelastic computations. *Comput. Methods. Appl. Mech. Eng.*, 134:71–90, 1996.
- [13] N.D. Melson, M.D. Sanetrik, and H.L. Atkins. Time-accurate Navier-Stokes calculations with multigrid acceleration. In *Proc. 6th Copper Mountain Confer. on Multigrid Methods*, 1993.
- [14] J.J. Sudirham, J.J.W. van der Vegt, and R.M.J. van Damme. Space-time discontinuous Galerkin method for advection-diffusion problems. Application to wet-chemical etching processes. *Appl. Numer. Mathematics (in press)*, 2006.
- [15] J.J.W. van der Vegt and H. van der Ven. Space-time discontinuous Galerkin finite element method with dynamic grid motion for inviscid compressible flows. I. General formulation. *J. Comput. Phys.*, 182:546–585, 2002.
- [16] H. van der Ven and J.J.W. van der Vegt. Space-time discontinuous Galerkin finite element method with dynamic grid motion for inviscid compressible flows. II. Efficient flux quadrature. *Comput. Meth. Appl. Mech. Engrg.*, 191:4747–4780, 2002.
- [17] H. van der Ven, J.J.W. van der Vegt, and E.G. Bouwman. Space-time discontinuous Galerkin finite element method for inviscid gas dynamics. In *Computational fluid and solid mechanics 2003 (MIT Boston)*, volume 1, pages 1181–1184. Elsevier Science, Oxford, UK., 2003.